CHALMERS

UNIVERSITY OF TECHNOLOGY

Impedance spectroscopy as a tool for moisture uptake monitoring in construction composites during service

(article starts on next page)

Impedance spectroscopy as a tool for moisture uptake monitoring in construction composites during service

Sotirios A. Grammatikos [a,*], Richard J. Ball [b], Mark Evernden [b], Ryan G. Jones [c]

[a] Department of Architecture and Civil Engineering, Chalmers University of Technology, Sweden
[b] Department of Architecture and Civil Engineering, University of Bath, United Kingdom
[c] Metros & Civil Division – Bridges, Mott MacDonald, Croydon, United Kingdom

ABSTRACT

This is a first study comparing dielectric spectroscopy and gravimetric measurements of moisture uptake in pultruded glass fibre reinforced polymers (FRPs). Specimens were subjected to sub-Tg hygrothermal aging for 224 days. Impedance spectra in the frequency range 0.1 Hz to 10 MHz were captured during exposure and compared with gravimetric measurements. Moisture concentration was found to increase the FRP's dielectric permittivity monotonically and decrease bulk resistance. High quality dielectric data was obtained as moisture uptake is independent of inherent changes suggested by mass loss which compromise gravimetry. Dielectric measurements remained sensitive to moisture despite significant mass loss, which typically distorts the weight gain process complicating the commonly adopted gravimetric methodology. Real-time dielectric measurements were obtained from FRP specimens continuously immersed in water and without making use of any additional sensing elements. The novel approach adopted is of high commercial impact as moisture uptake control is recognized as a significant problem by industry.

1. Introduction

Pultruded FRPs are commonly used materials in the civil engineering sector. They are usually employed as primary and secondary structural elements providing high resistance to extreme environmental conditions [1,2]. Compared to conventional engineering materials such as steel, FRPs possess high strength and stiffness-to-weight ratios as well as flexibility in the design of complex shapes [3–9]. In addition to bridge engineering, civil FRPs [10] are used in a variety of other engineering applications including facades, off-shore and on-shore platforms, wind turbine blades, ladders and composite utility poles [6,11,12], as well as reinforcement of concrete [13] and steel [14] structures.

It took many years for FRPs to enter the civil engineering market due to the increased manufacturing costs and lack of long-term service experience. The latter combined with the high retrofitting costs and the extensive maintenance regime has increased the need for efficient structural health monitoring in-service, which is crucial to the widespread adoption and safe design of FRP structures [15].

The primary cause of FRP structural degradation during service is environmental aging [15]. It has long been known that moisture absorbed during service has deleterious effects on FRPs' structural performance [1,15–17]. Absorbed moisture influences the electrical [18], physical, chemical and mechanical properties inducing both reversible and irreversible changes [19]. Reversible changes are physical, involving dimensional and mechanical property modifications [20]. Irreversible changes are attributed to chemical reactions resulting in permanent property changes. Matrix cracking, chain scission, residual cross-linking, hydrolysis, oxidation, softening and plasticization are the major effects of such moisture absorption [21,22]. In FRPs, moisture penetrates the surface and then diffuses and/or 'wicks' in the interior of the composite structure. Fibre/matrix interfacial loss reduces the adhesion between the fibre reinforcement and the matrix [23,24] enhancing interfacial capillary action by uncovering the reinforcement and therefore promoting fibre degradation. It has also been reported that moisture also attacks the fibre reinforcement itself, leading to significant mechanical property loss [25]. Capillary action or 'wicking' along the fibre reinforcement/matrix interface has been shown to be more pronounced than moisture diffusion within the composite matrix [26] which is verified by the higher amount of absorbed

* Corresponding author.
  E-mail address: grammatikos@outlook.com (S.A. Grammatikos).

moisture uptake in reinforced composites vs. plain resin polymers [27,28].

Water in composites can exist in different forms; free water molecules (unbound) which have diffused into the 'free-volume' from the outer surface of the composite, and water bound with the polymer matrix chain network [29]. Bound water is reported to induce the chemical interactions with the matrix compounds and is extremely difficult to be removed after drying [30–32]. Moisture concentration increases with time and reaches a saturation point after an extended period of time which is always dependent on the exposure temperature, the type and thickness of the material. Generally, moisture absorption in polymer composites follows a Fickian diffusion trend [15]. However, Fickian theory is unable to describe the moisture diffusion process when significant mass loss due to chemical decomposition occurs simultaneously with moisture absorption [33]. Other models have also been documented to describe the moisture diffusion kinetics, such as the Langmuir model [34]. Fig. 1 depicts 3 moisture uptake vs. time curves that are representative of (a) a classical Fickian diffusion three-stage curve with no mass loss, (b) a diffusion curve affected by mass loss taking place, and, (c) a 'true' diffusion curve when mass loss takes place without affecting the moisture uptake measurements.

For the assessment of moisture absorption characteristics, the gravimetric methodology has been largely employed by many researchers in both fully immersed and humidity-exposed conditions [3,15,20,33,35,36]. However, interpretation of gravimetric data becomes challenging when swelling, polymer relaxation and chemical decomposition processes take place at the same time as moisture absorption [37]. Dimensional changes due to swelling differentiate the 'free-volume' [20]. Chemical decomposition results in significant mass loss. This mass loss, which stems from the initial dry mass of the material, masks the mass gain due to moisture absorption [33]. Here an innovative method of probing moisture absorption in polymer composites via Electrical Impedance Spectroscopy (EIS) [38,39] is presented. Impedance spectroscopy is efficiently employed to capture moisture ingress independently of mass loss. Preliminary experiments of the present work were published in [40]. Conventional EIS has been extensively used to study corrosion of metallic materials [41] and metal coatings [42]. Dielectric property measurements have been applied to monitor curing of polymer matrix composites [43,44],
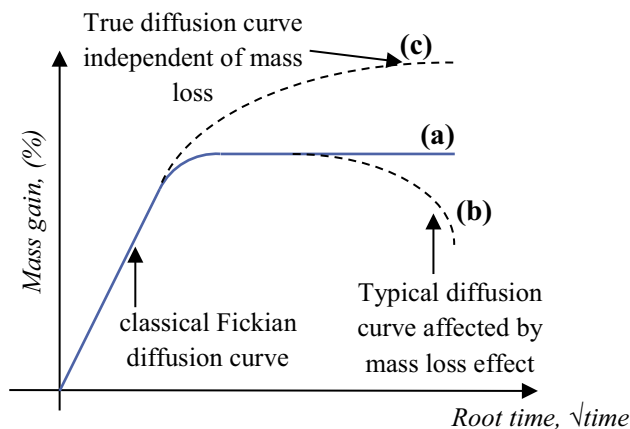
environmental degradation [45], damage [46–48] as well as the dispersion of nano-particles in polymer matrices [49,50]. Impedance spectroscopy measurements have been used to study moisture movement in mortar based construction materials [51,52] in addition to the more recent use in medical applications for moisture monitoring of wound dressings [53].

EIS is very sensitive to the presence of water due to the charge associated with the dipoles of water molecules [39,54]. Impedance measurements are expressed by the dielectric properties of the interrogated polymer composite coupled with the dielectric properties of the absorbed moisture [55]. The amount of moisture absorbed can be correlated directly with changes in the dielectric properties of the system. Impedance measurements involve the imposition of an AC potential field in a capacitor-like form. This field polarizes both the polymer and the water molecules (dipole polarization of the polar groups) inducing a frequency dependent displacement.

Maffezzoli et al. have used dielectric measurements to monitor water uptake characteristics in epoxy resin materials exposed to hygrothermal environments. Permittivity changes were used to determine moisture diffusion coefficient values and were evaluated against conventional gravimetric measurements. However, quantitative measurements of water uptake were not feasible. In the same work, an embedded dielectric sensor was adopted to record permittivity changes of samples that had to be removed from the aging medium for measurement [56]. Fraga et al. studied moisture uptake in polyester matrix glass [57] and jute [58] reinforced composites via the dielectric response and gravimetric measurements. Again, the interrogated samples were removed from the aging baths for the mass and dielectric measurements to be recorded. An increase in dielectric constant with moisture absorption was observed. Estimation of diffusion coefficient was also performed. However, quantitative measurements of moisture content were not made. Maxwell et al. studied the dielectric response of epoxy resin absorbing moisture over extremes of temperature (−60 °C to 70 °C) and distinguished the effect between 'unbound' and 'bound' water [59]. It was found that the behavior of dielectric conductivity is correlated with the water's molecular mobility. Chauffaille et al. applied electrical impedance spectroscopy to measure moisture uptake characteristics in thin polymeric adhesive films [39]. Moisture diffusion coefficient and moisture content were measured by bonding thin aluminum sheets to the polymeric film to act as measuring electrodes. In this work a methodology for permittivity suggested by Brasher and Kingsbury in 1954 was adopted [60]. Davis et al. demonstrated similar studies in adhesively bonded joints [55] as well as CFRP-reinforced concrete structures. Moisture ingress increases the amount of polar molecular fragments (contribution of both the large dipolar character and high mobility of polymer molecules) and therefore increases further the permittivity and phase delay [61,62]. As a consequence of the presence of mobile water dipoles, the overall conductivity of the exposed material is expected to increase at higher values of moisture ingress [63].

Although, it has been evident that impedance spectroscopy is sensitive to the presence of moisture or changes in moisture content, it is challenging to ascribe changes in impedance measurements to changes in moisture content alone. The dielectric properties of a polymer-water system are influenced by the nature of interaction between the water molecules (bound or unbound), the interrogated material, the polarization of the tested material and the surrounding system, the measuring electrodes as well as the electrical properties of the interrogated system as a whole. These parameters play a significant role in the dielectric measurements. Since dielectric changes are strongly associated with changes in moisture content, they carry important information that may be utilized as an efficient indicator of characteristics

Fig. 1. Representative plot of (a) a classical Fickian diffusion three-stage curve with no mass loss, (b) a diffusion curve affected by mass loss and (c) a 'true' diffusion curve when mass loss takes place without affecting moisture uptake measurements for *Mass gain* (%) vs. $\sqrt{t}$. (For interpretation of the references to colour in this figure legend, the reader is referred to the web version of this article.)

and properties which would otherwise be impossible to detect with the existing gravimetric experimental techniques.

This paper describes an innovative tool based on EIS for the monitoring of moisture absorption in a commercially available composite engineering material in real time. The proposed technique is presented through a complementary study based on gravimetric measurements revealing the superiority of EIS to efficiently capture moisture uptake characteristics. The EIS tool is aimed to be used in the field for capturing moisture uptake characteristics during service. Specimens were fully immersed in tap water at 60 °C in a thermostatically-controlled water tank. Metallic electrodes were applied to parallel faces of each specimen forming a capacitor, capable of capturing the dielectric property changes of the material during exposure. Samples were immersed in water continuously with connections allowing the dielectric data to be measured in-situ without the need of removing the samples. Moisture uptake measurements were extracted from the impedance data and plotted against gravimetric measurements to reveal; (i) the effectiveness of impedance spectroscopy to determine moisture uptake characteristics, and (ii) the mass loss effect which masks the moisture uptake measurements and thus the validity of gravimetry. The comparative study is apart from proposing a new tool, enhancing our understanding on the moisture uptake characteristics of pultruded FRP composites. This paper is part of an extensive study regarding the effects of moisture on the durability of polymer composites (DURACOMP project, Providing Confidence in Durable Composites, EP/K026925/1, EPSRC).

2. Experimental procedure

2.1. Material

A 5-ply commercially available glass FRP pultruded profile [FS040.101.096A] was studied provided by 'Creative Pultrusions Inc., PA, USA'. The nominal thickness of the profile was approximately 6.4 mm. The outer surfaces of the laminates were covered with an additional protecting and non-structural polyester veil providing the dual functions of retarding moisture ingress and protecting the PFRP material from UV radiation. E-glass fibres served as the reinforcement and an isophthalic polyester resin formed the matrix of the composite. Fig. 2 shows the structure of the tested FRP material which consisted of 3 continuous strand mats (CSM) and 2 unidirectional (UD) layers with 33.3% fibre and 54.5% fibre volume fractions, respectively.

2.2. Preparation of samples for dielectric measurements

To facilitate dielectric measurements, ∼1mm flat copper sheets were bonded at the outer plane surfaces of the 40×20×6.4 mm FRP samples. The following steps were followed for the preparation of the AC electrical contacts: (i) light abrasion of the plane surfaces with an emery cloth, (ii) thorough cleaning with distilled water, (iii) application of silver conductive paint on the abraded surfaces, (iv) bonding of copper sheets with silver adhesive paste, (v) soldering of cables (leads) to provide electrical continuity with the impedance analyzer and (vi) sealing of the copper sheets and cables with a thick epoxy layer to prevent short-circuits. The dielectric setup is schematically presented in Fig. 3. Samples are shown to be continuously immersed in the water medium and always connected to the impedance analyzer through cables. The two metallic plates form the capacitor required to obtain the dielectric measurements.

In the author's previous study on the hygrothermal aging at 60 °C [33], it was reported that the moisture content of the interrogated FRP at equilibrium is dependent on both the sample-size and sample-configuration. It was found that the examined FRP reaches a maximum moisture content at equilibrium that ranges from 1.82% to 2.34% per weight, for square samples with dimensions of 40 × 40 mm, 80 × 80mm and 200 × 200 mm [33]. This variation was attributed to the effects of significant mass loss due to leaching, during hygrothermal exposure, stemming from the fibre/matrix interfacial area [64].

2.3. Testing procedure

2.3.1. EIS measurements

EIS measurements were conducted using a Numetric PSM3750 impedance analyzer (Newtons 4th Ltd, UK). N4L software was used for data acquisition. As Fig. 3 illustrates, leads soldered in the middle of the outer surface of the copper sheets (that covered the sides of the specimens) providing connection with the impedance analyzer. A double epoxy layer and aluminum tape were used on top of the copper sheets to prevent moisture ingress/loss and contact with the water medium. All interrogated samples were oven-dried at 30 °C for 72 h in order to expel absorbed moisture from the environment prior to immersion in the water tank (Grant, UK) at 60 °C. During recording of the aforementioned dielectric measurements, the samples remained immersed in the water medium, i.e. they were not removed. Frequency scans were undertaken from 0.1 Hz to 10 MHz at prescribed time intervals for a maximum of 247 days. Impedance data was collected in 64 steps during the frequency sweep at an excitation voltage of 30 mV. The excitation voltage follows the following form:

$$E_t = E_o \sin(\omega t) \tag{1}$$

where E_t is the voltage at time t, E_o the amplitude of voltage (signal) and ω the radial frequency. The radial frequency is expressed as:
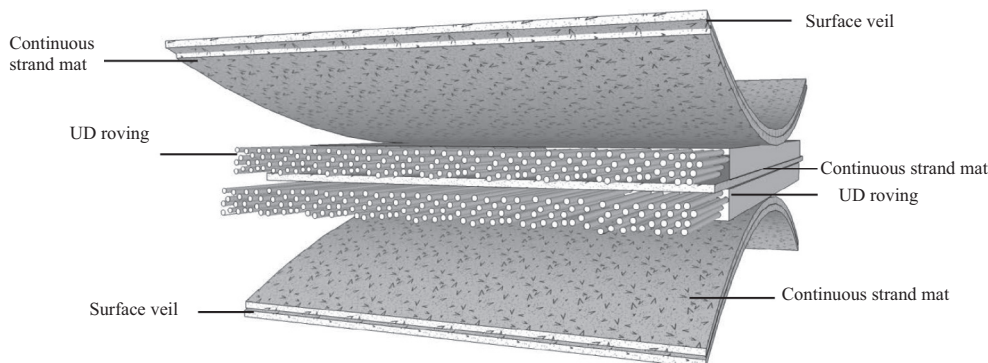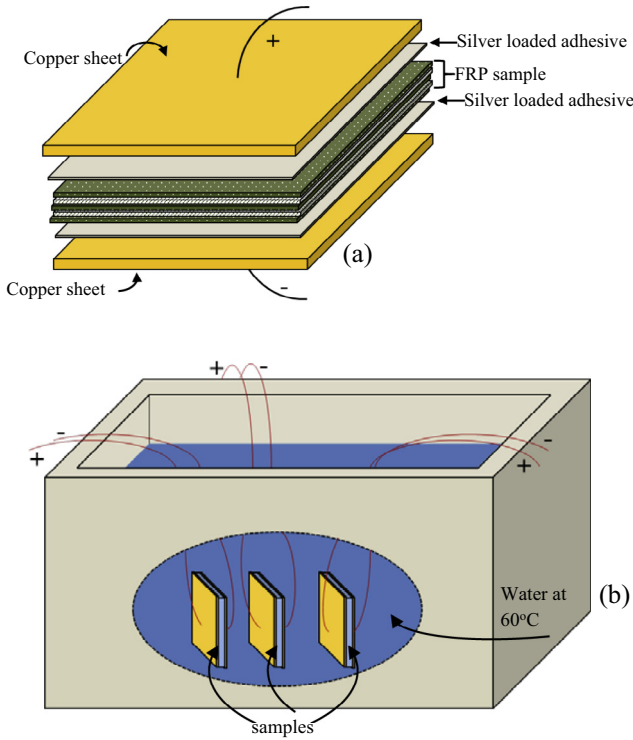
$$\omega = 2\pi f \tag{2}$$

Fig. 2. FRP profile schematic representation.

Fig. 3. Schematic representation of the experimental setup. (a) sample and (b) water tank. (For interpretation of the references to colour in this figure legend, the reader is referred to the web version of this article.)

where f is the frequency. For a linear system the response signal is shifted in phase Φ and has difference amplitude I_o:

$$I_t = I_o \sin(\omega t + \varphi) \tag{3}$$

Therefore, through the Ohm's law we may calculate the impedance of the system Z:

$$Z = \frac{E_t}{I_t} = \frac{E_o \sin(\omega t)}{I_o \sin(\omega t + \varphi)} = Z_o \frac{\sin(\omega t)}{\sin(\omega t + \varphi)} \tag{4}$$

and by making use of Euler's relationship, impedance can be expressed as a complex number:

$$Z(\omega) = \frac{E}{I} = Z_o \exp(j\Phi) = Z_o(\cos\Phi + j\sin\Phi) = Z' + iZ'' \tag{5}$$

where Z is the total impedance of the system, Z' the real and Z'' imaginary components of impedance, given as:

$$Z' = |Z|\cos\Phi \tag{6}$$

$$Z'' = |Z|\sin\Phi \tag{7}$$

where $|z|$ is the magnitude of the impedance expressed as:

$$|Z| = \sqrt{(Z')^2 + (Z'')^2} \tag{8}$$

The electrical impedance is usually represented by the complex dielectric permittivity, ε^*, which is expressed by the dielectric permittivity and the dielectric loss of the system:

$$\varepsilon^*(\omega) = \varepsilon'(\omega) + i\varepsilon''(\omega) \tag{9}$$

Dielectric permittivity (ε') is the real part of the permittivity and represents the ability of a material to store energy, while the dielectric loss (ε'') is the imaginary part of the permittivity which is associated with energy dissipation phenomena [56,65]. The real part of permittivity is calculated using Eq. (10):

$$\varepsilon' = -\frac{Z''}{Z'^2 + Z''^2} \cdot \frac{h}{\omega A \varepsilon_o} \tag{10}$$

where h is thickness, A is the area, ω is the angular frequency, and ε_o the electrical permittivity of free space. Fig. 4 illustrates a schematic representation of the dipoles yielded from both the FRP and the absorbed water molecules which polarize according to the direction of the electrical field.

Experimental data was modelled by using an equivalent electrical circuit that simulates the dielectric behavior/profile of the interrogated material during hygrothermal exposure. Equivalent circuit modelling was developed using Zman Impedance Spectroscopy Analysis software (Zive Zman, Korea). The circuit adopted was proposed by Davis et al. [38,66] for modelling the dielectric behavior of FRP composites (Fig. 5). Other more complicated circuits provided better fitting in most cases, but they could not comply with the parameters of the circuit. Given the gradual diffusion of water inside the FRP material, impedance spectra alter with aging time and therefore no single equivalent circuit was suitable for all the captured spectra. However, the simple circuit that was adopted in this study was found to generally provide acceptable output parameters and hence was considered suitable for modelling. The fitting quality was evaluated using the Nyquist and Bode plots. Fig. 5 illustrates the equivalent circuit used here.

2.3.2. Gravimetric measurements

Gravimetric measurements were conducted parallel to the impedance measurements. Samples were weighed using a digital analytical scale of 0.001 mg accuracy. Relative (M (%)) moisture uptake increase was determined using Eq. (11) (ASTM D5229):

$$M\ (\%) = \frac{M_t - M_0}{M_0} * 100\% \tag{11}$$

where M_t is the measured moisture mass at time t and M_o the initial dry mass (reference state). Moisture uptake measurements were conducted over a period up to 224 days [67]. For calculation of the moisture diffusion coefficient, Fickian theory (Fick's 2nd law) is commonly employed assuming uniform moisture and temperature conditions inside the material:

$$\frac{\partial x}{\partial t} = D \frac{\partial^2 C}{\partial x^2} \tag{12}$$

where x the is the distance along the thickness (h) of the material, the concentration of the water (C) and the diffusion coefficient value (D) [68]. Moisture absorption and diffusion processes are functions of temperature, the type of the material, fibre orientation and the fibre volume fraction [69,70].

Assuming that classical Fickian diffusion takes place, the diffusion coefficient (D) is calculated for the initial linear part of the moisture uptake vs. time curve as shown in Fig. 6. The slope of the linear part is given by:

$$Slope = \frac{M_2 - M_1}{\sqrt{t_2} - \sqrt{t_1}} \tag{13}$$

In classical Fickian behavior, diffusion coefficient is a constant parameter with respect to moisture concentration and temperature exposure. Typically, prolonged exposure induces deviation from the classical Fickian diffusion process and non-Fickian diffusion might take place [36,68].

From Eq. (12), according to [68], the solution for the 1D case is:

$$\frac{M_t}{M_\infty} = 1 - \frac{8}{\pi^2} \sum_{k=0}^{\infty} \frac{1}{(2k+1)^2} \exp\left(-\frac{D(2k+1)^2 \pi^2 t}{h^2}\right) \tag{14}$$

Subsequently, Eq. (14) can be simplified for short and long-term approximations, respectively:
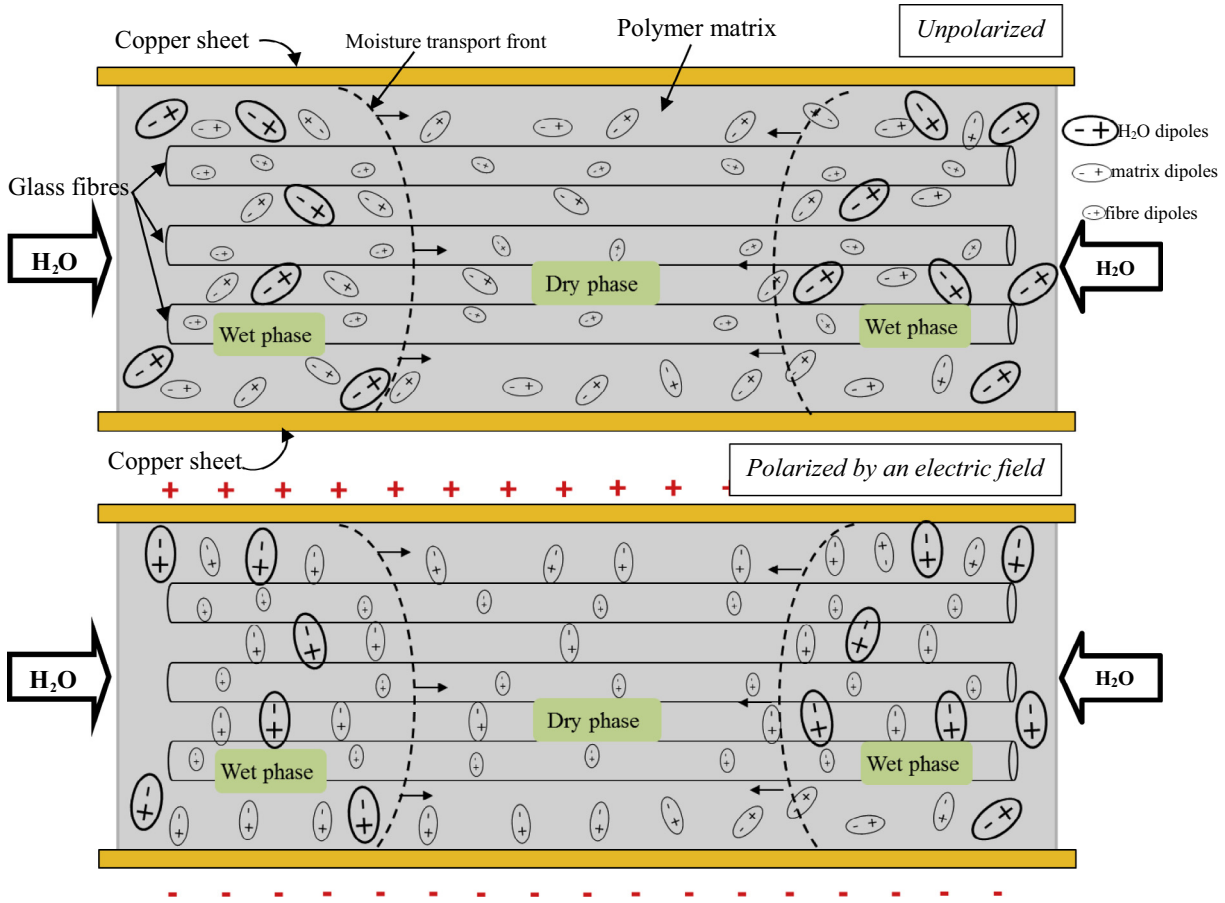
Fig. 4. Orientation of charged particles creating polarization effects. (For interpretation of the references to colour in this figure legend, the reader is referred to the web version of this article.)
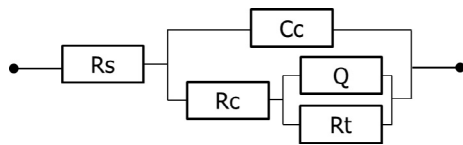

Fig. 5. Adopted equivalent electrical circuit; Rs = solution resistance, Rc = pore resistance, Q = constant phase element, Rt = interfacial resistance, Cc = capacitance.

Fig. 6. Diagram of a classical Fickian diffusion three-stage curve for $M(t)$ vs. $\sqrt{t}$ and the maximum absorbed moisture content M_∞. (For interpretation of the references to colour in this figure legend, the reader is referred to the web version of this article.)

$$\frac{M_t}{M_\infty} = \frac{4}{\pi^2} \sqrt{\frac{Dt}{h^2}} \quad \text{for } Dt/h^2 < 0.04 \tag{15}$$

$$\frac{M_t}{M_\infty} = 1 - \frac{8}{\pi^2} \exp\left(\frac{-Dt}{h^2}\pi^2\right) \quad \text{for } Dt/h^2 < 0.04. \tag{16}$$

As long as M_∞ can be established from a gravimetric curve (Fig. 6), D for a statistical homogeneous material can be determined using the following expression and two points of the moisture uptake M_1 and M_2 at times t_1 and t_2: (Fig. 6):

$$D = \pi \left(\frac{h}{4M_\infty}\right)^2 \left(\frac{M_2 - M_1}{\sqrt{t_2} - \sqrt{t_1}}\right)^2 \left(1 + \frac{h}{l} + \frac{h}{w}\right)^{-2} \tag{17}$$

where l and w represent length and width of the sample respectively. In Eq. (17) moisture diffusion process is assumed to occur mostly in the thickness direction. The final dimensional parameter in Eq. (17) accounts for the contribution in moisture absorption through the (cross-section) edges of the material [36]. It should be noted that, due to the peculiarity of the EIS testing, the case-tailored samples have mainly the cross-sectional edges exposed to water. This practically alters the kinetics of moisture absorption with respect to a real scenario, that of a fully exposed FRP sheet.

3. Results and discussion

3.1. EIS analysis

The subjection of a dielectric material/medium to an external AC electric field triggers its intrinsic atomic and molecular charges
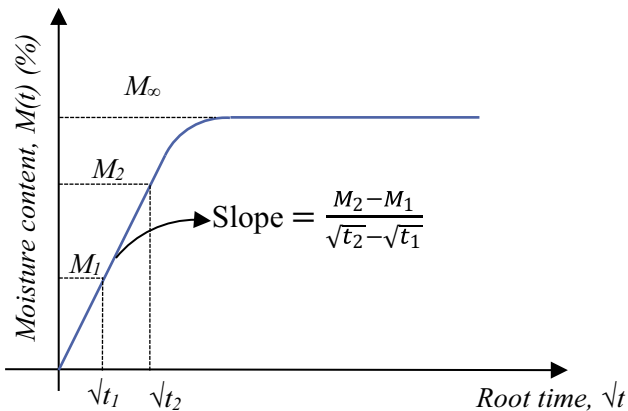
to polarize according to the direction of the applied external field. In this respect, the dielectric behavior of the material (susceptibility to dielectric polarization) is modified when water molecules penetrate the initially dry structure, thereby rendering their presence detectable. Absorbed water molecules will expectedly have an impact on the (i) dielectric permittivity (permittivity of air is lower than the permittivity of water) and (ii) magnitude of impedance (water is more electrically conductive than air).

Fig. 7 displays a 3-dimensional Nyquist plot for a representative sample aged for 224 days in water at 60 °C. After a reference spectrum was taken (before immersion-dry state), frequency sweeps were recorded at distinct time frames over the course of the aging period. Impedance measurements were acquired without removing the samples from the water tank. Inspection of the Nyquist plot reveals an arc (semicircle) possessing a single time constant which is indicative of a strong capacitive element which is deescalated with respect to the moisture uptake (aging time). Furthermore, the radius of the arc exhibits a monotonic depression with aging time which corresponds to the reduction of resistance of the system. This is attributed to the combined electronic polarization of the polymer composite influenced by the presence and concentration of the water molecules.

The presence of water within the FRP composite affects both the real and imaginary components of the impedance data. The real component is decreased due to enhancement of the system conductivity which can be attributed to the presence of the highly conductive water molecules, and the imaginary part of the impedance is decreased as the quantity of penetrated water increases, thus minimizing the inertia effects and the energy losses. Data collected at low frequencies in the transient state are attributed to the influence of the electrode leads connected to the samples. The increased magnitude of the recorded impedance shown in the Nyquist (Z' vs. Z'') plots, was mainly due to the electrochemical state of the polyester matrix. This behavior was similar to conductive-particle reinforced materials [71,72]. Fig. 8 depicts a 2-dimensional Nyquist plot for the same sample. The real (Z') and imaginary (Z'') parts of impedance were also fitted employing the equivalent electrical circuit manifested in Fig. 5. As can be seen, the adopted equivalent
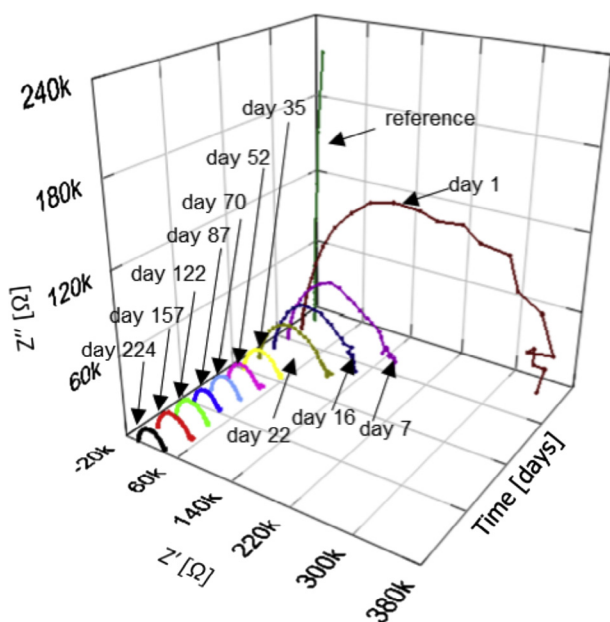
electrical circuit, shown by solid lines, efficiently simulates the impedance data and also allows for the subsequent efficient determination of various dielectric features of the polymer composite system under investigation such as electrical permittivity. The recorded semicircles describe the effect of dipolar polarization, driven by the absorbed water molecules within the polymer composite structure. The water molecules possess significantly higher values of permittivity increasing the mobility of the charge carriers (dielectric activity) of the interrogated system. The dielectric response of the material is thus dominated by the presence of the absorbed water molecules. The amount of water molecules has a cumulative effect on the dielectric response of the system forming a conductive network within the composite structure. This cumulative effect is manifested by the reduction in the bulk resistivity of the recorded system or the equivalent increase in the recorded permittivity values.
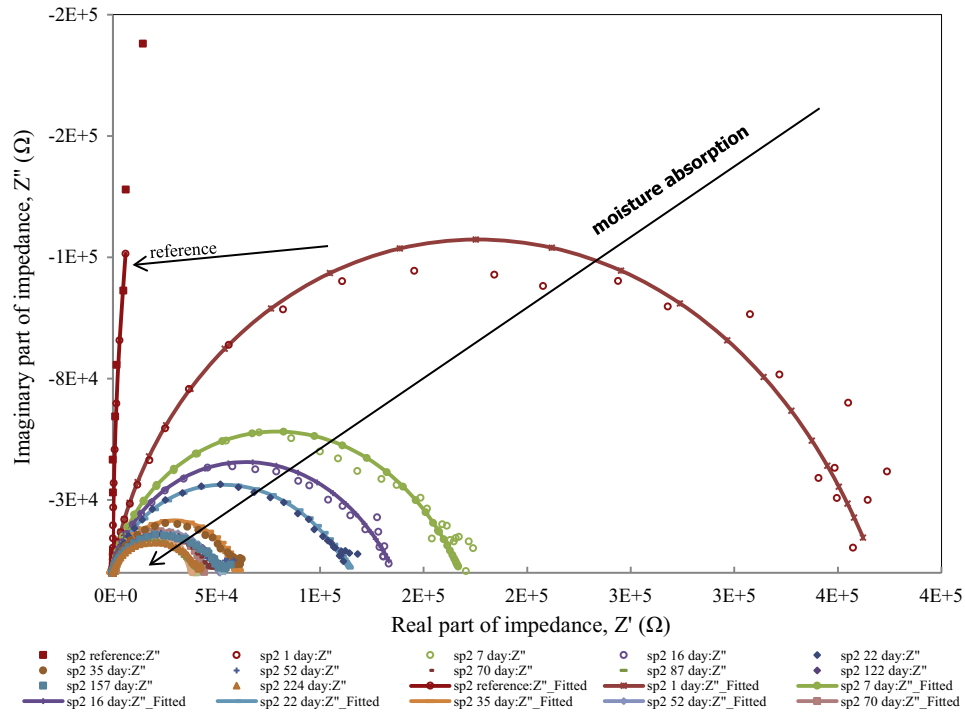
The calculated dielectric permittivity is attributed to all the dielectric properties between the electrodes/copper sheets; the polymer composite material and the moisture concentration that is absorbed filling intrinsic air gaps. Since the dielectric permittivity of the water molecules is significantly higher than that of air, the increase in the recorded permittivity of the system shown in Fig. 9 can be directly attributed to the presence of water molecules. It is well known that the presence of moisture in eoxy based FRPs may result to softening, swelling, and in some cases plasticization of the matrix [64]. Therefore, a small fraction of the absorbed water molecules may ultimately be bound to the polymer chains, as hygrothermal aging proceeds, gradually increasing the mobility of the polymer chains. Increased polymer chain mobility is likely to modify the electrical signature of the polymer matrix itself in the long run (irreversible plasticization). Fraga et al. [73] proposed a relationship that describes the dynamic dependence of electrical permittivity on the relative changes in water concentration and polymer chain mobility. Any intricacies of the potential change in the electrical signature of the composite when hygrothermally aged are here being neglected. As shown in Fig. 9, dielectric permittivity decreases at higher frequencies (irrespective of the moisture content), but increases as moisture concentration increases.

Fig. 10 depicts the development of the magnitude of impedance during hygrothermal exposure. After a very high reference value recorded for the dry state, impedance values were then dominated by the presence and accumulation of water molecules inside the structure of the polymer composite. It is worth noting that at low frequencies the measurement of the magnitude of impedance for the dry reference state was unstable and therefore only data greater than $\sim 10^3$ Hz are considered. A distinct impedance transition phase is evident in the frequency spectrum between 10^3 and 10^4 Hz where the ohmic behavior of the material changes to purely capacitive and frequency-dependent while the material fails to impede the imposed electric field. In addition, as the concentration of water increases, the transition frequency where hysteretic phenomena occur, shifts towards higher frequencies of the impedance spectrum. This effect can be attributed to the increased mobility of charged carriers and their ability to follow the variations of the external field even in high frequencies.

3.2. Moisture uptake characteristics

In this section, a quantifying analysis of the findings of the impedance spectroscopy readings is presented. Impedance spectroscopy data were analyzed with a view to determining the exact moisture uptake characteristics i.e. moisture content absorbed by the polymer composite during hygrothermal exposure.

In parallel to the impedance measurements, gravimetric measurements were conducted. A second set of samples (5 in total) of identical configuration and dimensions to that of the impedance

Fig. 7. Nyquist plot of the real and imaginary parts of impedance for a period of 224 days. (For interpretation of the references to colour in this figure legend, the reader is referred to the web version of this article.)

Fig. 8. Nyquist plot of the imaginary and real parts of the impedance for 224 days. (For interpretation of the references to colour in this figure legend, the reader is referred to the web version of this article.)
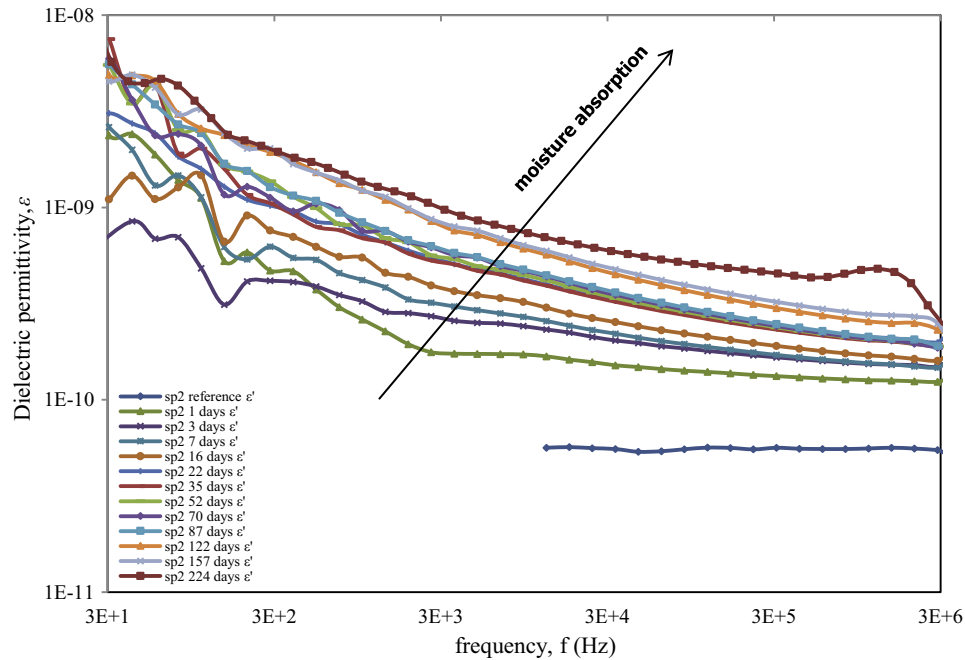
Fig. 9. Recorded dielectric permittivity vs. frequency for 224 days. (For interpretation of the references to colour in this figure legend, the reader is referred to the web version of this article.)

test samples, were hot/wet aged under identical conditions by recording their weight for a period of 224 days according to the procedure described in Section 2.3.

With respect to the impedance spectroscopy data, moisture uptake characteristics were determined by adopting the procedure reported by Davis et al. [55]. For the determination of the relative moisture uptake increase (M (%)), the following equation was used:

$$M\ (\%) = \frac{\frac{C}{C_i} - 1}{\varepsilon_w/\varepsilon_{comp}} = 0.047\left(\frac{C}{C_i} - 1\right) \tag{18}$$
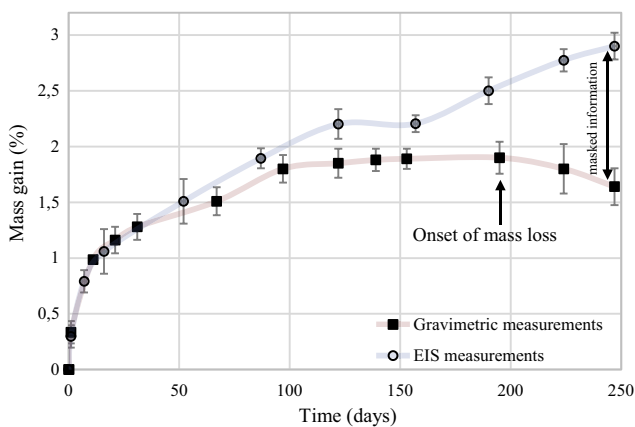
where C_i is the initial (reference) capacitance of the material recorded at the dry state before exposure, C the capacitance of the material at a given time stage, ε_w the dielectric permittivity of water and ε_{comp} the dielectric permittivity of the composite.
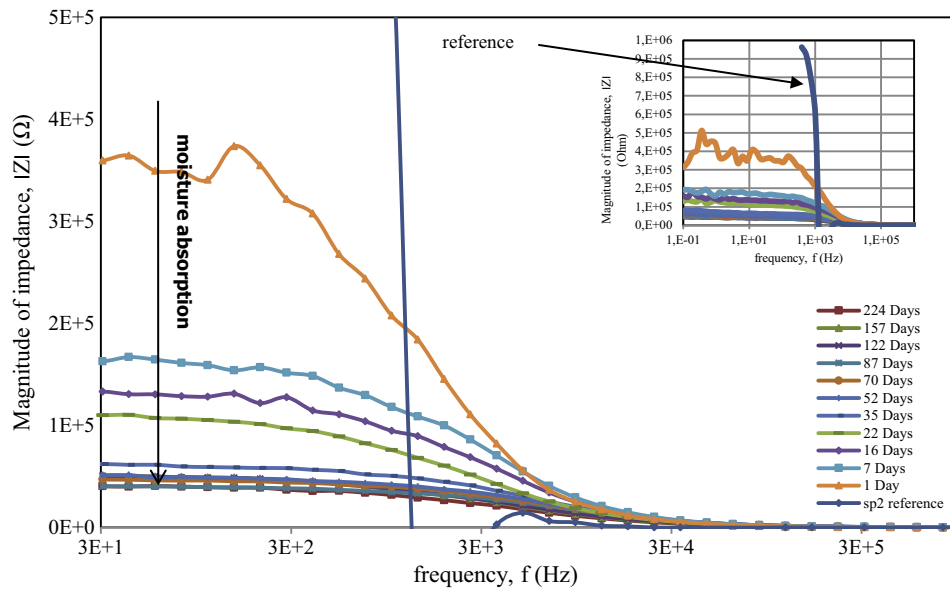
Fig. 10. Recorded magnitude of real impedance vs. frequency for 224 days. (For interpretation of the references to colour in this figure legend, the reader is referred to the web version of this article.)

Fig. 11 depicts a comparison of the experimental findings via the gravimetric and electrical impedance methodologies. Water uptake is plotted as a function of time for the samples aged in water for more than 224 days. The y-axis represents the M (%) derived from Eq. (1) for the gravimetry (marked with blank circles) and Eq. (18) for the impedance spectroscopy (marked with filled squares), while the x-axis is a linear scale of time in days. From the author's previous work, samples of the same material aged at 60 °C reached a maximum of 2.34% moisture content, by mass, for 40×40 mm^2 samples, after 224 days over the course of which samples had lost 1% of their initial dry mass due to leaching (chemical decomposition) [33]. Here, samples reached a maximum of 1.9% and 2.9%, for the gravimetric and dielectric measurements, respectively, thereby revealing the effectiveness of EIS as a replacement for gravimetry in FRP testing. It can be seen in Fig. 11, mass gain measured with gravimetry reaches a maximum at 1.9% (aging day 195) and then decreases with time to 1.64% after 224 days, due to significant mass loss. On the contrary, mass gain monitored with impedance spectroscopy, keeps increasing even after 224 days, indicating that 'true' moisture uptake lasts longer than that suggested via gravimetry while saturation has not yet been reached [74]. It is known that when moisture penetrates a polymer composite, it induces chemical decomposition which leads to substantial mass loss, masking the gravimetric measurements of moisture absorption. Along with mass loss, matrix cracking and fibre/matrix interfacial failure are highly likely to increase the internal 'reservoir' for more water molecules to penetrate. The latter effect goes undetected when conventionally recording the weight gain of the aged FRP samples. On the other hand, impedance spectroscopy, being independent of mass loss, is thus capable of capturing the 'true' moisture uptake during aging as dielectric measurements are only dependent on the differences in permittivity between air-gaps and water molecules. Therefore, impedance spectroscopy can be employed as a smart tool for 'true' moisture uptake monitoring in polymer composites that undergo chemical decomposition as well as in real applications of construction polymer composites during service.

It should be noted that since EIS deals with the electrical profile of the material, it is possible that the electrical measurements will be affected by the wet environment surrounding the location of measurement. For the fully immersed case (like the one here), assuming that the water medium is infinite, any possible electrical leakage may be considered as a relatively constant factor in all measurements, without problematically complicating the overall recording of the EIS readings. However, significant fluctuations in the service environment (i.e. absorption–desorption cycles, etc.) might influence the EIS data and such an effect should be taken into account and calibrated.

4. Concluding remarks

Pultruded FRP composites are prone to swelling, polymer relaxation and chemical decomposition when subjected to severe environmental conditions. Chemical decomposition leads to mass loss of the initial dry mass, as a result of effective ion leaching. An investigation of moisture uptake characteristics of such composites with the conventional gravimetric methodology, usually fails, due to the lack of appropriate interpretation means of this significant mass loss exhibited by weight measurements.

Fig. 11. Moisture uptake vs. time calculated with gravimetry (weight measurements) and impedance spectroscopy. (For interpretation of the references to colour in this figure legend, the reader is referred to the web version of this article.)

This study proposes EIS, as an efficient solution for monitoring moisture uptake characteristics of construction pultruded FRP composites. The proposed methodology captures changes in the dielectric behavior of the FRPs caused by the presence of moisture. The study was conducted on a commercially available pultruded FRP sheet, fully immersed in water at 60 °C. To explore the effectiveness of the proposed system, the EIS measurements were contradicted with gravimetric data recorded in parallel. The dielectric properties were captured in real time without removing the samples from the water tank which is not the case for gravimetry. Gravimetric measurements revealed that moisture saturation was reached after 224 soaking days. After that, gravimetric measurements were shown to be largely affected by mass loss due to leaching. On the other hand, hygrothermal exposure induced somehow linear changes to the dielectric properties such as magnitude of impedance and electrical permittivity. Moisture uptake was shown to continue beyond the point at which it was not measured by gravimetry. This confirmed the high sensitivity of impedance measurements to moisture absorption but also the independency of significant mass loss due to chemical decomposition when using EIS. Also, it is highly likely that mass loss increased the intrinsic space available within the material to absorb water molecules, contributing to a further marginal increase of moisture content and subsequent change in dielectric properties. Thus, mass loss masks the true moisture absorption when measured with gravimetry, which fails to capture the resulting secondary moisture absorption effects.

In conclusion, impedance spectroscopy, independent of mass loss, is capable of capturing the 'true' moisture uptake during environmental exposure since dielectric measurements are only dependent on permittivity differences between air and water molecules. Impedance spectroscopy can be employed as an efficient tool for the study of moisture uptake characteristics of FRP composites in laboratory environments as well as in field applications of construction FRPs.

Acknowledgements

References

[1] Pochiraju KV, Tandon GP, Schoeppner GA. Long-term durability of polymeric matrix composites, Springer; 2011.

[2] Karbhari V, Chin J, Hunston D, Benmokrane B, Juska T, Morgan R, et al. Durability gap analysis for fiber-reinforced polymer composites in civil infrastructure. J Compos Constr 2003;7(3):238–47.

[3] Correia JR, Cabral-Fonseca S, Branco FA, Ferreira JG, Eusébio MI, Rodrigues MP. Durability of pultruded glass-fiber-reinforced polyester profiles for structural applications. Mech Compos Mater 2006;42(4):325–38.

[4] Plevris N, Triantafillou T. FRP-reinforced wood as structural material. J Mater Civ Eng 1992;4(3):300–17.

[5] Davalos JF, Qiao P, Frank XuX, Robinson J, Barth KE. Modeling and characterization of fiber-reinforced plastic honeycomb sandwich panels for highway bridge applications. Compos Struct 2001;52(3–4):441–52.

[6] Price JC. The "State of the Art" in composite material development and applications for the oil and gas industry. Int Soc Offshore Polar Eng.

[7] Mara V, Haghani R, Harryson P. Bridge decks of fibre reinforced polymer (FRP): a sustainable solution. Constr Build Mater 2014;50:190–9.

[8] Zhou A, Tam L-H, Yu Z, Lau D. Effect of moisture on the mechanical properties of CFRP–wood composite: an experimental and atomistic investigation. Compos B Eng 2015;71:63–73.

[9] Front matter. In: Hollaway LC, Teng JG, editors. Strengthening and rehabilitation of civil infrastructures using Fibre-Reinforced Polymer (FRP) composites, Woodhead Publishing; 2008. p. i–iii.

[10] Bakis C, Bank L, Brown V, Cosenza E, Davalos J, Lesko J, et al. Fiber-reinforced polymer composites for construction—state-of-the-art review. J Compos Constr 2002;6(2):73–87.

[11] The New and Improved PultexÒ Pultrusion Design Manual. In: Inc. CP, editor. Alum Bank, PA2014. p. 255.

[12] Shao Y, Kouadio S. Durability of fiberglass composite sheet piles in water. J Compos Constr 2002;6(4):280–7.

[13] Retrofitting by use of FRP. Solid Mechanics and its Applications; 2016. p. 83–96.

[14] Linghoff D, Haghani R, Al-Emrani M. Carbon-fibre composites for strengthening steel structures. Thin-Walled Struct 2009;47(10):1048–58.

[15] Surathi P, Karbhari VM. Project SSR, University of California SDDoSE, Services CDoTDoE. Hygrothermal Effects on Durability and Moisture Kinetics of Fiber-reinforced Polymer Composites: Department of Structural Engineering, University of California, San Diego; 2006.

[16] Bank LC, Gentry TR, Barkatt A. Accelerated test methods to determine the long-term behavior of FRP composite structures: environmental effects. J Reinf Plast Compos 1995;14(6):559–87.

[17] Maxwell AS, Broughton WR, Dean G, Sims G. Review of accelerated ageing methods and lifetime prediction techniques for polymeric materials. National Physical Laboratory; 2005.

[18] Apicella A, Egiziano L, Nicolais L, Tucci V. Environmental degradation of the electrical and thermal properties of organic insulating materials. J Mater Sci 1988;23(2):729–35.

[19] Environmental Degradation of Industrial Composites. In: Mahieux CA, editor. Environmental Degradation of Industrial Composites. Oxford: Elsevier Science; 2005. p. xi-xviii.

[20] Starkova O, Buschhorn ST, Mannov E, Schulte K, Aniskevich A. Water transport in epoxy/MWCNT composites. Eur Polym J 2013;49(8):2138–48.

[21] Schoeppner GA, Tandon GP, Pochiraju KV. Predicting Thermooxidative Degradation and Performance of High-Temperature Polymer Matrix Composites. In: Kwon Y, Allen D, Talreja R, editors. Multiscale modeling and simulation of composite materials and structures, Springer US; 2008. p. 359–462.

[22] Kumar BG, Singh RP, Nakamura T. Degradation of carbon fiber-reinforced epoxy composites by ultraviolet radiation and condensation. J Compos Mater 2002;36(24):2713–33.

[23] Joliff Y, Belec L, Heman MB, Chailan JF. Experimental, analytical and numerical study of water diffusion in unidirectional composite materials – interphase impact. Comput Mater Sci 2012;64:141–5.

[24] Akay M, Ah Mun SK, Stanley A. Influence of moisture on the thermal and mechanical properties of autoclaved and oven-cured Kevlar-49/epoxy laminates. Compos Sci Technol 1997;57(5):565–71.

[25] Hinkley J, Connell J. Resin systems and chemistry: degradation mechanisms and durability. In: Pochiraju KV, Tandon GP, Schoeppner GA, editors. Long-term durability of polymeric matrix composites: Springer US; 2012. p. 1–37.

[26] Liao K, Schultheisz CR, Hunston DL. Effects of environmental aging on the properties of pultruded GFRP. Compos B Eng 1999;30(5):485–93.

[27] Lassila LVJ, Nohrström T, Vallittu PK. The influence of short-term water storage on the flexural properties of unidirectional glass fiber-reinforced composites. Biomaterials 2002;23(10):2221–9.

[28] Morii T, Tanimoto T, Hamada H, Maekawa Z-i, Hirano T, Kiyosumi K. Weight changes of a randomly orientated GRP panel in hot water. Compos Sci Technol 1993;49(3):209–16.

[29] Zhou J, Lucas JP. Hygrothermal effects of epoxy resin. Part II: Variations of glass transition temperature. Polymer 1999;40(20):5513–22.

[30] Papanicolaou GC, Xepapadaki AG, Zarouchas DS. Effect of water uptake on creep behaviour of glass–epoxy composites. Plast, Rubber Compos 2009;38(2–4):72–9.

[31] Papanicolaou GC, Kosmidou TV, Vatalis AS, Delides CG. Water absorption mechanism and some anomalous effects on the mechanical and viscoelastic behavior of an epoxy system. J Appl Polym Sci 2006;99(4):1328–44.

[32] Mouzakis DE, Zoga H, Galiotis C. Accelerated environmental ageing study of polyester/glass fiber reinforced composites (GFRPCs). Compos B Eng 2008;39(3):467–75.

[33] Grammatikos SA, Zafari B, Evernden MC, Mottram JT, Mitchels JM. Moisture uptake characteristics of a pultruded fibre reinforced polymer flat sheet subjected to hot/wet aging. Polym Degrad Stab 2015;121:407–19.

[34] Carter HG, Kibler KG. Langmuir-type model for anomalous moisture diffusion in composite resins. J Compos Mater 1978;12(2):118–31.

[35] He Y. In-situ characterization of moisture absorption-desorption and hygroscopic swelling behavior of an underfill material. In: Proceedings - electronic components and technology conference; 2011. p. 375–86.

[36] Shen C-H, Springer GS. Moisture absorption and desorption of composite materials. J Compos Mater 1976;10(1):2–20.

[37] Berens AR, Hopfenberg HB. Diffusion and relaxation in glassy polymer powders: 2. Separation of diffusion and relaxation parameters. Polymer 1978;19(5):489–96.

[38] Davis GD, Rich MJ, Drzal LT. Monitoring moisture uptake and delamination in CFRP-reinforced concrete structures with electrochemical impedance sensors. J Nondestr Eval 2004;23(1):1–9.

[39] Chauffaille S, Devos O, Jumel J, Shanahan MER. Liquid diffusion in polymeric adhesives by electrochemical-impedance spectroscopy (EIS). Int J Adhes Adhes 2010;30(7):602–8.

[40] Grammatikos SA, Evernden M. Effects of hygrothermal aging on pultruded glass fibre reinforced polymers: a complimentary study. Advanced Composites in Construction. In: ACIC 2015 – Proceedings of the 7th Biennial conference on advanced composites in construction; 2015. p. 109–14.

[41] Mansfeld F, Kendig MW, Tsai S. Recording and analysis of ac impedance data for corrosion studies – 2. Experimental approach and results. Corrosion (Houston); 1982;38(11):570–80.

[42] Murray JN. Electrochemical test methods for evaluating organic coatings on metals: an update. Part III: Multiple test parameter measurements. Prog Org Coat 1997;31(4):375–91.

[43] Gkikas G, Saganas C, Grammatikos SA, Aggelis DG, Paipetis AS. Simultaneous acoustic and dielectric real time curing monitoring of epoxy systems. In: Proceedings of SPIE – The International Society for Optical Engineering; 2012.

[44] O'Dwyer MJ, Maistros GM, James SW, Tatam RP, Partridge IK. Relating the state of cure to the real-time internal strain development in a curing composite using in-fibre Bragg gratings and dielectric sensors. Meas Sci Technol 1998;9 (8):1153–8.

[45] Bekas D, Grammatikos SA, Kouimtzi C, Paipetis AS. Linear and non-linear electrical dependency of carbon nanotube reinforced composites to internal damage. In: IOP Conference Series: Materials Science and Engineering, 1 ed.; 2015.

[46] Raihan R, Adkins JM, Baker J, Rabbi F, Reifsnider K. Relationship of dielectric property change to composite material state degradation. Compos Sci Technol 2014;105:160–5.

[47] Bekas DG, Paipetis AS. Study of the effect of damage on the electrical impedance of carbon nanotube reinforced epoxy nanocomposites. J Sens 2015;2015.

[48] Bekas DG, Paipetis AS. Damage monitoring in nanoenhanced composites using impedance spectroscopy. Compos Sci Technol 2016;134:96–105.

[49] Gkikas G, Saganas C, Grammatikos SA, Maistros GM, Barkoula NM, Paipetis AS. Dispersion monitoring of carbon nanotube modified epoxy systems. In: Proceedings of SPIE – the international society for optical engineering; 2012.

[50] Bekas DG, Gkikas G, Maistros GM, Paipetis AS. On the use of dielectric spectroscopy for the real time assessment of the dispersion of carbon nanotubes in epoxy. RSC Adv 2016;6(82):78838–45.

[51] Ball RJ, Allen GC, Starrs G, McCarter WJ. Impedance spectroscopy measurements to study physio-chemical processes in lime-based composites. Appl Phys A 2011;105(3):739–51.

[52] Ball RJ, Allen GC. The measurement of water transport in porous materials using impedance spectroscopy. J Phys D Appl Phys 2010;43(10):105503.

[53] McColl D, Cartlidge B, Connolly P. Real-time monitoring of moisture levels in wound dressings in vitro: an experimental study. Int J Surg 2007;5(5):316–22.

[54] Boinard P, Banks WM, Pethrick RA. Changes in the dielectric relaxations of water in epoxy resin as a function of the extent of water ingress in carbon fibre composites. Polymer 2005;46(7):2218–29.

[55] Davis GD, Pethrick RA, Doyle J. Detection of moisture in adhesive bonds using electrochemical impedance and dielectric spectroscopies. J Adhes Sci Technol 2009;23(4):507–28.

[56] Maffezzoli AM, Peterson L, Seferis JC, Kenny J, Nicolais L. Dielectric characterization of water sorption in epoxy resin matrices. Polym Eng Sci 1993;33(2):75–82.

[57] Fraga AN, Frullloni E, De La Osa O, Kenny JM, Vázquez A. Relationship between water absorption and dielectric behavior of glass fiber reinforced unsaturated polyester resin. J Compos Mater 2007;41(4):393–402.

[58] Fraga AN, Frullloni E, De La Osa O, Kenny JM, Vázquez A. Relationship between water absorption and dielectric behaviour of natural fibre composite materials. Polym Test 2006;25(2):181–7.

[59] Maxwell ID, Pethrick RA. Dielectric studies of water in epoxy resins. J Appl Polym Sci 1983;28(7):2363–79.

[60] Brasher DM, Kingsbury AH. Electrical measurements in the study of immersed paint coatings on metal. I. Comparison between capacitance and gravimetric methods of estimating water-uptake. J Appl Chem 1954;4(2):62–72.

[61] Fukuda A, Mitsui H, Inou Y, Goto K. Influence of water absorption on dielectric properties of cycloaliphatic epoxy resin. Proceedings of the IEEE international conference on properties and applications of dielectric materials; 1997. p. 58–61.

[62] Karner HC, Ieda M. Technical aspects of interfacial phenomena in solid insulating systems; 1992. p. 592–7.

[63] Li Y, Cordovez M, Karbhari VM. Dielectric and mechanical characterization of processing and moisture uptake effects in E-glass/epoxy composites. Compos B Eng 2003;34(4):383–90.

[64] Grammatikos SA, Evernden M, Mitchels J, Zafari B, Mottram JT, Papanicolaou GC. On the response to hygrothermal aging of pultruded FRPs used in the civil engineering sector. Mater Des 2016;96:283–95.

[65] Barsoukov E, Macdonald JR. Impedance spectroscopy: theory, experiment, and applications. Wiley; 2005.

[66] Davis GD, Krebs LA, Drzal LT, Rich MJ, Askeland P. Electrochemical sensors for nondestructive evaluation of adhesive bonds. J Adhes 2000;72(3–4):335–58.

[67] Bank LC, Gentry TR, Thompson BP, Russell JS. A model specification for FRP composites for civil engineering structures. Constr Build Mater 2003;17(6–7):405–37.

[68] Crank J. The mathematics of diffusion. Clarendon Press; 1975.

[69] Rao RMVGK, Balasubramanian N, Chanda M. Factors affecting moisture absorption in polymer composites. Part I: Influence of internal factors. J Reinforced Plast Compos 1984;3(3):232–45.

[70] Rao RMVGK, Chanda M, Balasubramanian N. Factors affecting moisture absorption in polymer composites. Part II: Influence of external factors. J Reinforced Plast Compos 1984;3(3):246–53.

[71] Ford SJ, Shane JD, Mason TO. Assignment of features in impedance spectra of the cement-paste/steel system. Cem Concr Res 1998;28(12):1737–51.

[72] Torrents JM, Mason TO, Peled A, Shah SP, Garboczi EJ. Analysis of the impedance spectra of short conductive fiber-reinforced composites. J Mater Sci 2001;36(16):4003–12.

[73] Fraga AN, Alvarez VA, Vazquez A, de la Osa O. Relationship between dynamic mechanical properties and water absorption of unsaturated polyester and vinyl ester glass fiber composites. J Compos Mater 2003;37(17):1553–74.

[74] Chin JW, Aouadi K, Haight MR, Hughes WL, Nguyen T. Effects of water, salt solution and simulated concrete pore solution on the properties of composite matrix resins used in civil engineering applications. Polym Compos 2001;22 (2):282–97.